MATHEMATICAL MODELING AND COMPUTING, Vol. 9, No. 2, pp. 365–374 (2022)

Low-rank tensor completion using nonconvex total variation

Mohaoui S., El Qate K., Hakim A., Raghay S.

Cadi Ayyad University, Faculty of Science and Technics, Guiliz, Marrakesh, Morocco

(Received 16 June 2021; Accepted 2 April 2022)

In this work, we study the tensor completion problem in which the main point is to predict the missing values in visual data. To greatly benefit from the smoothness structure and edge-preserving property in visual images, we suggest a tensor completion model that seeks gradient sparsity via the l_0-norm. The proposal combines the low-rank matrix factorization which guarantees the low-rankness property and the nonconvex total variation (TV). We present several experiments to demonstrate the performance of our model compared with popular tensor completion methods in terms of visual and quantitative measures.

Keywords: *tensor completion, missing values, parallel matrix factorization, nonconvex TV.*

2010 MSC: 34A34, 65L05 **DOI:** 10.23939/mmc2022.02.365

1. Introduction

Low-rank tensor completion is the task of filling missing entries in incomplete multidimensional data. As for the matrix case, the rank function is a powerful tool to capture some type of global information. However, a basic issue in the low-rank tensor completion is the definition of the tensor rank which is not unique [1] as for the matrix rank. The tensor nuclear norm which is based on extending the definition of the matrix nuclear norm to the tensor case has been widely used to define the convex surrogate of the tensor rank. A central drawback of the nuclear norm-based algorithms is calculating the singular value decomposition in each iteration, which suffers from high computational costs. To cope with this problem, [2] proposed another efficient model which performs low-rank property using parallel matrix factorization by unfolding the current tensor. Parallel matrix factorization has demonstrated its effectiveness for tensor recovery [3] especially in filling with missing values in multidimensional data [2, 4, 5]. In the last models, the use of additional prior knowledge that characterize the local information in the reconstruction problem has been advantageous.

The theory of regularization plays a crucial role in the image procesing area [6–10]. Total variation (TV) regularization is an efficient regularizer that has been widely used to explore the piecewise smoothness structure of data, due to its advantageous edge-preserving property. Although it has initially proposed for the denoising context [11], it has nonetheless been successfully adapted to various applications. For low-rank tensor completion, total variation defined by l_1 TV has introduced to exploit the spectral smoothness along the third dimension [4, 5]. Those methods have achieved remarkable performance. However, they only exploit the spectral smoothness and ignore the spatial piecewise structure exhibited in the first and the second modes. Besides, the convex l_1-TV penalizes the large gradient magnitudes which may affect the preservation of the image edges. Therefore, to efficiently preserve more information, a novel l_0 based TV has been introduced in [12].

In this paper, we present a novel completion model based on a nonconvex penalty of the original tensor. In addition to the parallel low-rank matrix factorization, the spectral-spatial smoothness property characterized by nonconvex l_0-total variation is exploited. The l_0 gradient penalty counts the number of nonzero gradients. This choice is motivated by the fact that the l_0 gradient penalization can give rise to truly piecewise structure and better enhance highest-contrast edges by confining the number of nonzero gradients [12].

2. Preliminaries

2.1. Notation on tensor

In this subsection, we introduce basic notation on tensors and definitions used through the rest of this paper. We use Euler script for denoting tensors e.g. $\mathcal{X}$ and upper-case letters for matrices e.g. X. A tensor $\mathcal{X}$ is a multi-dimensional structure in $\mathbb{R}^{I_1 \times I_2 \times \ldots \times I_N}$.

Mode-i unfold: It may be convenient to store N-way arrays in matrices. This transformation is called matrix unfolding.

Mode-i unfold of the tensor $\mathcal{X}$ is denoted as

$$X_{(i)} = \mathbf{unfold}(\mathcal{X}) \in \mathbb{R}^{I_i \times \hat{s}}, \tag{1}$$

where $\hat{s} = \prod_{k \neq i}^{N} I_k$, $X_{(i)}$ is a matrix with columns being the mode-i fibers of X in the lexicographical order.

The inverse operator of **unfold** is denoted as **fold** and defined as follows:

$$\mathcal{X} = \mathbf{fold}_i(X_{(i)}). \tag{2}$$

The tensor **rank** is defined as $\mathbf{rank}(\mathcal{X}) = \big(\text{rank}(X_{(1)}, \text{rank}(X_{(2)}, \ldots, \text{rank}(X_{(N)})\big)$. The tensor $\mathcal{X}$ is low-rank, if $X_{(i)}$ is low rank for all i.

Definition 1 (Mixed $l_{1,0}$ pseudo-norm). *For a given vector $\mathbf{y} \in \mathbb{R}^m$ and index sets $s_1, \ldots, s_i, \ldots, s_n$ $(1 \leqslant n \leqslant m)$ that satisfies the following properties:*

— *each s_i is a subset of $1, \ldots, m$,*
— *$s_i \cap s_l = \varnothing$ for any $i \neq l$,*
— *$\cup_{i=1}^{n} s_i = 1, \ldots, m$*

the mixed $l_{1,0}$ pseudo-norm of y is defined as:

$$\|\mathbf{y}\|_{1,0}^{s} = \|(\|\mathbf{y}_{s_1}\|_1, \ldots, \|\mathbf{y}_{s_1}\|_1, \ldots \|\mathbf{y}_{s_n}\|_1)\|_0 \tag{3}$$

where $\mathbf{y}_{s_i}$ denotes a sub-vector of $\mathbf{y}$ with its entries specified by s_i and $\|\cdot\|_0$ calculates the number of the non-zero entries in $(\cdot)$.

Definition 2 (Indicator function). *Let $\mathcal{B}$ be a given operator and γ be a positive fixed integer, the indicator function of $l_{1,0}$ mixed pseudonorm is defined as follows*

$$I_{\|\mathcal{B}\cdot\|_{1,0}^{s}}(y) = \begin{cases} 0, & \|\mathcal{B}\mathbf{y}\|_{1,0}^{s} \leqslant \gamma, \\ \infty, & \textit{otherwise}. \end{cases} \tag{4}$$

3. Low-rank tensor completion problem

According to current research, the effective recovery of matrix and tensor completeness is mostly dependent on their low-rank assumption [13,14]. The rank function is an effective method for capturing global data. As a result, we frequently assume that the matrix or tensor is low-rank or nearly so. The direct minimization of the tensor rank and the updating of the low-rank tensor is a typical method for the completion problem,

$$\begin{aligned} &\min_{\mathcal{Y}} \text{rank}(\mathcal{Y}) \\ &\text{s.t. } \mathcal{P}_{\Omega}(\mathcal{Y}) = \mathcal{F}, \end{aligned} \tag{5}$$

where $\mathcal{Y} \in \mathbb{R}^{n_1 \times n_2 \times n_3}$ is the recovered tensor, $\mathcal{F}$ is the observed data, and $\mathcal{P}_{\Omega}$ denotes the projection of $\mathcal{Y}$ on the observed set Ω (the random sampling operator) which is defined by

$$\mathcal{P}_{\Omega}(\mathcal{Y}) = \begin{cases} \mathcal{Y}_{i_1, i_2, \ldots, i_n} & \text{if } \ (i_1, i_2, \ldots, i_n) \in \Omega, \\ 0 & \text{otherwise}. \end{cases}$$

Several models for the tensor completion problem have been proposed depending on the definition of the tensor rank. The rank($\mathcal{Y}$) operator has different forms, such as CANDECOMP/PARAFA (CP) rank [1] and Tucker rank. Actually, the rank minimization problem suffers from different issues. First, it is a non-convex function and the problem (5) is NP-hard. Thus, analog to the matrix case, the nuclear norm is then used as the convex surrogate of the rank function. However, the definition of the nuclear norm of a tensor still a complicated issue since it cannot be intuitively derived from the matrix case. Different versions of tensor nuclear norms have been proposed. Liu et al. [15] first proposed a tensor completion approach based on the sum of matricized nuclear norms (SMNN) of the tensor. However, nuclear norm-based models make use of the singular values decomposition which is known to be expensive in terms of computational cost. Thus, a recent version of the tensor nuclear norm is the matrix factorization model which stands on the approximation of each matricization tensor of the underlying tensor by two low-rank factors .

4. The proposed model

To better characterize and enhance important components in a given visual data, we propose a sparsity-based gradient regularization in addition to the low-rank matrix factorization for the tensor completion problem. The gradient-based priors have extensively exploited in several image processing applications, owing to their ability to suppress artifacts and ameliorate the reconstructed images effectively. The sparsity property is naturally obtained via the l_0-norm which simply counts the number of nonzero elements in a vector. In the gradient domain, the l_0-norm counts the amplitude changes discretely.

4.1. The sparse l_0-gradient

The l_0 regularized gradient can control the number of non-zero gradients globally. Unlike existing edge-preserving smoothing methods, this prior knowledge does not rely on local characteristics but instead locates important edges. The l_0 total variation has been proposed for 2D image deblurring [16] and has been recently extended to the tensorial framework for hyperspectral images denoising [12]. Motivated by the promising results presented by those models, we make use of the l_0-gradient penalty in the context of tensor completion. It is defined as follows:

$$l_0\mathrm{TV}(\mathcal{X}) = \sum_i^h \sum_j^v C\left(\sum_k^z \left(|\mathcal{X}_{i+1,j,k} - \mathcal{X}_{i,j,k}| + |\mathcal{X}_{i,j+1,k} - \mathcal{X}_{i,j,k}|\right)\right), \tag{6}$$

where $C(X)$ is a binary function that simply counts how may non-zeros image gradients which is defined as follows

$$C(X) := \begin{cases} 1, & \text{if} \quad X \neq 0, \\ 0, & \text{otherwise,} \end{cases} \tag{7}$$

where boundary values of gradients are defined as follows

$$\begin{cases} \mathcal{X}_{i,j+1,k} - \mathcal{X}_{i,j,k} = 0, & \text{if} \quad i = h, \\ \mathcal{X}_{i+1,j,k} - \mathcal{X}_{i,j,k} = 0, & \text{if} \quad j = v. \end{cases} \tag{8}$$

Actually, the $l_0\mathrm{TV}(\mathcal{X})$ counts the non-zeros gradients in the spatial dimension with the assistance of spectral information. With definition 1, another formulation of the l_0-TV becomes:

$$l_0\mathrm{TV}(\mathcal{X}) = \|\mathcal{B}D\mathcal{X}\|_{1,0}^s, \tag{9}$$

where operator D is an operator to calculate both horizontal and vertical differences. Operator $\mathcal{B}$ is an operator that forces boundary values of gradients to be zero when $i = h$ and $j = v$.

4.2. Nonconvex TV for tensor completion

To better exploit the aforementioned properties, we propose an alternative completion model formulated as the following nonconvex minimization problem

$$\begin{aligned} &\min_{A,X,\mathcal{Y}} \sum_{n=1}^{N} \frac{\alpha_n}{2} \left\| Y_{(n)} - A_n X_n \right\|_F^2 \\ &\text{s.t. } \|BD\mathcal{Y}\|_{1,0}^{s} \leqslant \gamma \quad \text{and} \quad \mathcal{P}_\Omega(\mathcal{Y}) = \mathcal{F}, \end{aligned} \tag{10}$$

where $A = (A_1, A_2, \ldots, A_N)$, $X = (X_1, X_2, \ldots, X_N)$, $\alpha_n \geqslant 0$ $(n = 1, 2, \ldots, N)$, and $\sum_{n=1}^{N} \alpha_n = 1$.

4.3. Alternating minimization-based solving algorithm

Considering a three-way tensor $\mathcal{Y} \in \mathbb{R}^{n_1 \times n_2 \times n_3}$, the Lagrangian function associated to the proposed model (10) is given as

$$\min f(A, X, \mathcal{Y}) = \min_{A,X,\mathcal{Y}} \sum_{n=1}^{N} \frac{\alpha_n}{2} \left\| Y_{(n)} - A_n X_n \right\|_F^2 + I_{\|\mathcal{B}\cdot\|_{1,0}^{s}}(D\mathcal{Y}) + \iota(\mathcal{Y}), \tag{11}$$

where τ and λ are regularization parameters, and $\iota(\cdot)$ is the following indicator function:

$$\iota(\mathcal{Y}) := \begin{cases} 0, & \text{if} \quad \mathcal{P}_\Omega(\mathcal{Y}) = \mathcal{F}, \\ \infty, & \text{otherwise}. \end{cases} \tag{12}$$

Within the framework of Alternating Minimization-based algorithm, the problem (11) can be solved by updating the three subproblems alternately

$$\begin{cases} \text{Step 1: } A^{k+1} = \operatorname{argmin}_A f(A, X^k, \mathcal{Y}^k), \\ \text{Step 2: } X^{k+1} = \operatorname{argmin}_X f(X^{k+1}, X, \mathcal{Y}^k), \\ \text{Step 3: } \mathcal{Y}^{k+1} = \operatorname{argmin}_{\mathcal{Y}} f(A^{k+1}, X^{l+1}, \mathcal{Y}), \end{cases} \tag{13}$$

which is equivalent to the following two basic steps

$$\begin{cases} \text{Step 1: } \left(A^{k+1}, X^{k+1}\right) = \operatorname{argmin}_{A,X} \sum_{n=1}^{N} \frac{\alpha_n}{2} \left\| Y_{(n)} - A_n X_n \right\|_F^2, \\ \text{Step 2: } \mathcal{Y}^{k+1} = \operatorname{argmin}_{\mathcal{Y}} \sum_{n=1}^{N} \frac{\alpha_n}{2} \left\| Y_{(n)} - A_n X_n \right\|_F^2 + I_{\|\mathcal{B}\cdot\|_{1,0}^{s}}(D\mathcal{Y}) + \iota(\mathcal{Y}). \end{cases} \tag{14}$$

4.3.1. (X, A)-subproblem

Since the objective function of the X-subproblem is strictly quadratic, the problem has a closed form solution. Set the partial derivative of the function over X to zero yield the following linear equation:

$$X_n^{k+1} = \left((A_n^k)^T A_n^k\right)^{\dagger} \left((A_n^k)^T Y_{(n)}^k\right), \quad n = 1, 2, 3. \tag{15}$$

Similar to the minimization of X-subproblem, the closed-from solution of A is given by the following linear equation:

$$A_n^{k+1} = \left(Y_{(n)}^k (X_n^{k+1})^T\right) \left(X_n^{k+1} (X_n^{k+1})^T\right)^{\dagger}, \quad n = 1, 2, 3. \tag{16}$$

4.3.2. $\mathcal{Y}$-subproblem

In contrast to the above minimization subproblems, the minimization of the $\mathcal{Y}$-subproblem can be computationally challenging. A popular method to solve it, is to decouple the problem using variable slitting technique. By introducing an auxiliary variable noted $\mathcal{V}$, we can rewrite the $\mathcal{Y}$-subproblem as the following equivalent constrained problem

$$\begin{aligned} &\min_{X,A,\mathcal{Y}} \sum_{n=1}^{N} \frac{\alpha_n}{2} \left\| Y_{(n)} - A_n X_n \right\|_F^2 + I_{\|\mathcal{B}\cdot\|_{1,0}^{s}}(\mathcal{V}) + \iota(\mathcal{Y}) \\ &\text{s.t. } \mathcal{V} = D\mathcal{Y}. \end{aligned} \tag{17}$$

The augmented Lagrangian function associated to problem (17) can be expressed as follows:

$$L_\beta(\mathcal{Y},\mathcal{V},\mathcal{M})=\sum_{n=1}^{N}\frac{\alpha_n}{2}\left\|Y_{(n)}-A_nX_n\right\|_F^2+\frac{\beta}{2}\|\mathcal{V}-D\mathcal{Y}-\mathcal{M}/\beta\|_F^2+I_{\|\mathcal{B}\cdot\|_{1,0}^s}(\mathcal{V})+\iota(\mathcal{Y}), \tag{18}$$

where $\mathcal{M}$ are the Lagrange multipliers and $\beta>0$ is the penalty parameter. Problem (18), is then alternately minimized with respect to each block of variables $\mathcal{Y},\mathcal{V}$, and the Lagrangian multiplier $\mathcal{M}$

$$\begin{cases}\mathcal{Y}^{k+1,p+1}=\operatorname{argmin}_{\mathcal{Y}} L_\beta(\mathcal{Y},\mathcal{V}^p,\mathcal{M}^p),\\ \mathcal{V}^{p+1}=\operatorname{argmin}_{\mathcal{V}} L_\beta\left(\mathcal{Y}^{k+1,p+1},\mathcal{V},\mathcal{M}^p\right),\\ \mathcal{M}^{p+1}=\mathcal{M}^p+\beta\left(D\mathcal{Y}^{k+1,p+1}-\mathcal{V}^{p+1}\right),\end{cases} \tag{19}$$

which equivalent to

$$\begin{cases}\mathcal{Y}^{k+1,p+1}=\operatorname{argmin}_{\mathcal{Y}}\sum_{n=1}^{N}\frac{\alpha_n}{2}\left\|Y_{(n)}-A_nX_n\right\|_F^2+\frac{\beta}{2}\|\mathcal{V}^p-D\mathcal{Y}-\mathcal{M}^p/\beta\|_F^2+\iota(\mathcal{Y}),\\ \mathcal{V}^{p+1}=\operatorname{argmin}_{\mathcal{V}}\frac{\beta}{2}\|\mathcal{V}-D\mathcal{Y}^{k+1,p+1}-\mathcal{M}^p/\beta\|_F^2+I_{\|\mathcal{B}\cdot\|_{1,0}^s}(\mathcal{V}),\\ \mathcal{M}^{p+1}=\mathcal{M}^p+\beta\left(D\mathcal{Y}^{k+1,p+1}-\mathcal{V}^{p+1}\right).\end{cases} \tag{20}$$

1. Update $\mathcal{Y}$. The minimization over the $\mathcal{Y}$ has a closed form solution. Let Ω^c be the compliment of Ω, and the fact that $\mathcal{P}_{\Omega^c}(\mathcal{F})=0$ we obtain the following solution

$$\mathcal{Y}^{k+1,p+1}=\mathcal{P}_{\Omega^c}\left(\frac{\sum_{n=1}^{3}\alpha_n\,\mathbf{fold}_n\left(\alpha_nA_n^{k+1}X_n^{k+1}\right)+\beta D^T\mathcal{V}^p-\mathcal{M}^p/\beta}{1+\beta D^TD}\right)+\mathcal{F}. \tag{21}$$

2. Update $\mathcal{V}$. Actually, the sub-problem of $\mathcal{V}$ can be expressed by the following constrained minimization problem:

$$\begin{aligned}&\min_{\mathcal{V}}\|\mathcal{V}-D\mathcal{Y}^{k+1,p+1}-\mathcal{M}^{p+1}\|_F^2\\ &\text{s.t.}\quad \|B\mathcal{V}\|_{1,0}^s\leqslant\gamma.\end{aligned} \tag{22}$$

The resolution of problem (22) is performed by the following Proposition.

Theorem 1 (Projection onto $l_{1,0}$ mixed pseudo-norm ball with binary mask [17]). *Let $\mathbf{y}\in\mathbb{R}^m$ as a known vector and γ as a non-negative integer. Let $\mathbf{W}$ be a known diagonal binary matrix, and let $s_1,\dots,s_n(1\leqslant n\leqslant m)$ be index sets satisfying the conditions from definition 1. Without loss of generality, we can assume that $\mathbf{W}\mathbf{y}=\left(\mathbf{y}_{s_1}^T\dots\mathbf{y}_{s_n}^T\right)^T$. Additionally, we denote by the subvectors $\mathbf{y}_{s_{(1)}}\dots\mathbf{y}_{s_{(n)}}$ are sorted in descending order according to the l_2 norm: $\left\|\mathbf{y}_{s_{(1)}}\right\|_2\geqslant\left\|\mathbf{y}_{s_{(2)}}\right\|_2\geqslant\dots\geqslant\left\|\mathbf{y}_{s_{(n)}}\right\|_2$. The following problem*

$$\mathbf{z}^\star\in\underset{\mathbf{z}\in\mathbb{R}^M}{\operatorname{argmin}}\|\mathbf{y}-\mathbf{z}\|^2\quad\textit{subject to}\quad\|\mathbf{W}\mathbf{z}\|_{1,0}^s\leqslant\gamma$$

. has one of the optimal solutions

$$\mathbf{z}^\star=\begin{cases}\mathbf{y}, & \textit{if}\quad \|\mathbf{W}\|_{1,0}^s\leqslant\gamma,\\ \left(\overline{\mathbf{y}}_{s_1}^\top\cdots\overline{\mathbf{y}}_{s_n}^\top\right)^\top+(\mathbf{I}-\mathbf{W})\mathbf{y}, & \textit{if}\quad \|\mathbf{W}\|_{1,0}^s>\gamma,\end{cases}$$

where

$$\overline{\mathbf{y}}_{s_k}:=\begin{cases}\mathbf{y}_{s_k}, & \textit{if}\quad k\in\{(1),\dots,(\gamma)\},\\ \mathbf{0}, & \textit{if}\quad k\in\{(\gamma+1),\dots,(n)\}\end{cases}$$

Algorithm 1 Nonconvex tensor completion algorithm (NC_TC).

Require: The observed tensor $\mathcal{F}$, the set of index of observed entries Ω;
Ensure: The recovered tensor $\mathcal{Y}$;
1: initialization: $\mathcal{X} = \mathcal{F}$, A_n^0, Z_n^0 for $n = 1, 2, 3$;
2: **for** $k = 1, \ldots, \mathrm{nMax}$
3: **Low-rank matrix factorization step**
– update A_n^{k+1} for $n = 1, 2, 3$;
– update Z_n^{k+1} for $n = 1, 2, 3$;
4: **The tensor completion step**
– update the l_0 projection $\mathcal{V}^{k+1}$;
– update the reconstructed tensor $\mathcal{Y}^{k+1}$;
– update the lagrangian multiplier $\mathcal{M}^{k+1}$.

5. Experimental results

This section is devoted to the numerical results in which we evaluate the performance of the proposed Nonconvex completion algorithm. Thus, we conduct experiments on four benchmark 3D channel RGB color images. The missing values are distributed randomly. The accuracy of the obtained results are measured by the peak signal to noise ratio (PSNR) and structural similarity (SSIM).

Table 1. The PSNR/SSIM obtained by the completion of four images using different sampling ratios 10%, 20%, 30%, and 40%. For each test, the results of LRTC [18], TNNR [19], MF-TV [4], and our proposed NC-TC are illustrated and the best among the results is highlight in bold face.

SR	10%		20%		30%		40%	
Methods	PSNR	SSIM	PSNR	SSIM	PSNR	SSIM	PSNR	SSIM
				Image 1				
TNNR	24.31	0.6262	28.84	0.8190	31.55	0.8911	34.15	0.9362
LRTC	23.38	0.6007	28.41	0.8046	31.29	0.8859	33.89	0.9333
MF-TV	17.55	0.2083	28.38	0.8075	32.25	0.8869	**34.40**	0.9215
NC-TC	**29.18**	**0.8780**	**31.40**	**0.9159**	**33.01**	**0.9386**	34.25	**0.9548**
				Image 2				
TNNR	14.34	0.2336	17.93	0.4510	21.04	0.6088	24.01	0.7349
LRTC	13.84	0.2209	17.76	0.4415	20.76	0.5920	23.80	0.7206
MF-TV	8.838	0.1236	15.40	0.4063	15.87	0.3982	24.16	0.7011
NC-TC	**18.29**	**0.6256**	**20.90**	**0.7596**	**22.63**	**0.8314**	**24.23**	**0.8803**
				Image 3				
TNNR	19.69	0.3587	23.67	0.5893	26.36	0.7213	28.78	0.8147
LRTC	19.11	0.3295	23.40	0.5694	26.06	0.7029	28.57	0.8046
MF-TV	10.14	0.0401	17.38	0.3210	22.17	0.5187	28.65	0.7872
NC-TC	**24.47**	**0.7296**	**26.63**	**0.8127**	**28.33**	**0.8658**	**29.76**	**0.9006**
				Image 4				
TNNR	16.42	0.2351	20.69	0.4649	23.53	0.6171	26.06	0.7290
LRTC	15.56	0.2071	20.44	0.4489	23.21	0.7384	25.77	0.7127
MF-TV	9.987	0.0964	18.62	0.4235	23.53	0.5972	27.12	0.7751
NC-TC	**22.90**	**0.7370**	**25.33**	**0.8255**	**27.16**	**0.8749**	**28.80**	**0.9112**

Fig. 1. The visual comparison results of the recovered *Image 1*. From left to right and to bottom, the original image, the incomplete image with 30% of observation, the recovered results by TNNR, LRTC, MF_TV, and the proposed NC_TV respectively.

Fig. 2. The visual comparison results of the recovered *Image 2*. The original image, the incomplete image with 30% of observation,the recovered results by TNNR, LRTC, MF_TV, and the proposed NC_TV respectively.

Fig. 3. The visual comparison results of the recovered *Image 1*. The original image, the incomplete image with 30% of observation,the recovered results by TNNR, LRTC, MFTV, and the proposed NCTV respectively.

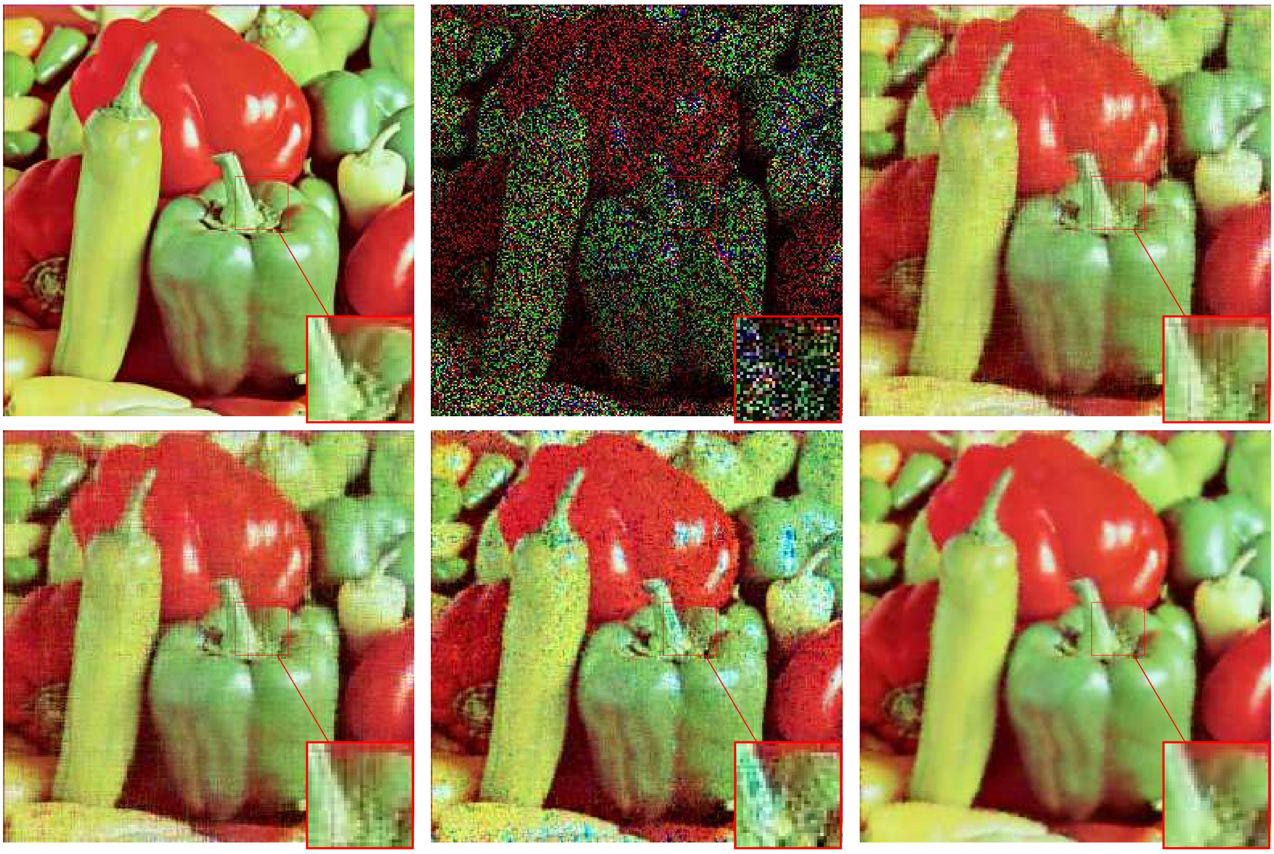

Fig. 4. The visual comparison results of the recovered *Image 4*. The original image, the incomplete image with 30% of observation,the recovered results by TNNR, LRTC, MF_TV, and the proposed NC_TV respectively.

We start the numerical results section by the comparison of the evaluation criterion. Therefore, we present in Table 1, the PSNR and SSIM values of the obtained results of different tests using the four images with different sampling ratios. Overall, we clearly observe that the proposed NC_TC model presents larger PSNR and SSIM values compared with three tensor completion methods. Besides, according to the PSNR and SSIM values, the MF_TV method presents poor completion results when the sampling ratio is very small (especially when SR=10%). In contrast, our approach demonstrates its effectiveness with respect to an extremely small set of observation.

To further show the significant impact of our algorithm on the completion of RGB color images, we visually compare the results of four tensor completion methods. Thus, in Figures 1, 2, 3, and Figure 4 we illustrate the reconstructed results obtained by using TNNR, LRTC, MF_TV and our proposed NC_TC model. For test images with 70% of missing values respectively. As can be seen, the proposed method can effectively predict the missing values in the images and thus provides more accurate completion results. More importantly, the reconstructed images obtained by the proposed NC_TC method contain more preserved information. Hence, we can conclude that NC_TC is robust and stable with respect to the sampling ratio.

6. Conclusion

We presented in this paper, a novel tensor completion model using sparse gradient regularization. In addition to the low-rankness information exhibited by the matrix factorization, the nonconvex total variation is exploited in order to globally estimate and enhance important edges. To validate the proposed algorithm, different experiments have been performed over the third-order tensor. The proposed method demonstrates an improvement in filling with missing values while preserving fundamental components in the target tensor.

[1] Kolda T. G., Bader B. W. Tensor decompositions and applications. SIAM review. **51** (3), 455–500 (2009).

[2] Xu Y., Hao R., Yin W., Su Z. Parallel matrix factorization for low-rank tensor completion. Preprint arXiv:1312.1254 (2013).

[3] He W., Zhang H., Zhang L., Shen H. Total-variation-regularized low-rank matrix factorization for hyperspectral image restoration. IEEE transactions on geoscience and remote sensing. **54** (1), 178–188 (2015).

[4] Ji T.-Y., Huang T.-Z., Zhao X.-L., Ma T.-H., Liu G. Tensor completion using total variation and low-rank matrix factorization. Information Sciences. **326**, 243–257 (2016).

[5] Jiang T.-X., Huang T.-Z., Zhao X.-L., Ji T.-Y., Deng L.-J. Matrix factorization for low-rank tensor completion using framelet prior. Information Sciences. **436–437**, 403–417 (2018).

[6] Ben-Loghfyry A., Hakim A. Time-fractional diffusion equation for signal and image smoothing. Mathematical Modeling and Computing. **9** (2), 351–364 (2022).

[7] Alaa H., Alaa N. E., Atounti M., Aqel F. A new mathematical model for contrast enhancement in digital images. Mathematical Modeling and Computing. **9** (2), 342–350 (2022).

[8] Alaa H., Alaa N. E., Aqel F., Lefraich H. A new Lattice Boltzmann method for a Gray-Scott based model applied to image restoration and contrast enhancement. Mathematical Modeling and Computing. **9** (2), 187–202 (2022).

[9] Mohaoui S., Hakim A., Raghay S. Bi-dictionary learning model for medical image reconstruction from undersampled data. IET Image Processing. **14** (10), 2130–2139 (2020).

[10] Mohaoui S., Hakim A., Raghay S. A combined dictionary learning and TV model for image restoration with convergence analysis. Journal of Mathematical Modeling. **9** (1), 13–30 (2021).

[11] Rudin L. I., Osher S., Fatemi E. Nonlinear total variation based noise removal algorithms. Physica D: Nonlinear Phenomena. **60** (1–4), 259–268 (1992).

[12] Wang M., Wang Q., Chanussot J. Tensor low-rank constraint and l_0 total variation for hyperspectral image mixed noise removal. IEEE Journal of Selected Topics in Signal Processing. **15** (3), 718–733 (2021).

[13] Banouar O., Mohaoui S., Raghay S. Collaborating filtering using unsupervised learning for image reconstruction from missing data. EURASIP Journal on Advances in Signal Processing. **2018**, 72 (2018).

[14] Mohaoui S., Hakim A., Raghay S. Tensor completion via bilevel minimization with fixed-point constraint to estimate missing elements in noisy data. Advances in Computational Mathematics. **47** (1), 10 (2021).

[15] Liu J., Musialski P., Wonka P., Ye J. Tensor completion for estimating missing values in visual data. IEEE transactions on pattern analysis and machine intelligence. **35** (1), 208–220 (2012).

[16] Xu L., Zheng S., Jia J. Unnatural l_0 sparse representation for natural image deblurring. 2013 IEEE Conference on Computer Vision and Pattern Recognition. 1107–1114 (2013).

[17] Ono S. l_0 gradient projection. IEEE Transactions on Image Processing. **26** (4), 1554–1564 (2017).

[18] Xue S., Qiu W., Liu F., Jin X. Low-rank tensor completion by truncated nuclear norm regularization. 2018 24th International Conference on Pattern Recognition (ICPR). 2600–2605 (2018).

[19] Wright J., Ganesh A., Rao S., Ma Y. Robust principal component analysis: Exact recovery of corrupted low-rank matrices via convex optimization. Advances in Neural Information Processing Systems 22 (NIPS 2009). **22** (2009).

Доповнення тензора низького рангу з використанням неопуклої повної варіації

Мохауї С., Ель Кате К., Хакім А., Рагей С.

Університет Каді Айяд, Факультет науки і техніки, Гіліз, Марракеш, Марокко

У цій роботі вивчається задача тензорного доповнення, в якій головним є передбачення відсутніх значень у візуальних даних. Щоб отримати максимальну користь із гладкої структури та властивості збереження країв у візуальних зображеннях, пропонується модель тензорного доповнення, яка шукає розрідженість градієнта за допомогою l_0-норми. Пропозиція поєднує в собі матричну факторізацію низького рангу, яка гарантує властивість низького рангу та неопуклі повні варіації (ПВ). Подано декілька експериментів, щоб продемонструвати ефективність запропонованої моделі порівняно з популярними методами тензорного доповнення з точки зору візуальних і кількісних показників.

Ключові слова: *тензорне доповнення, пропущені значення, паралельна матрична факторізація, неопукла ПВ.*